Ornate Setae on the Branchial Flabella ("Gill Rakers") of the Green Shore Crab *Carcinus maenas* (Crustacea: Decapoda)[1]

MICHAEL J. CAVEY, EESH MODI, AND JERREL L. WILKENS

Division of Zoology, Department of Biological Sciences, The University of Calgary, 2500 University Drive N. W., Calgary, Alberta T2N 1N4, Canada

Abstract. The branchial flabella ("gill rakers") of the green shore crab *Carcinus maenas* originate from the first three thoracopods. Each flabellum is a flattened blade that projects posteriorly to lie between the phyllobranchiate gills and the walls of the branchial chamber. Numerous setae emerge from cuticular depressions along the edges of the blade. These setae may be categorized on the basis of length: "long" setae are 3.72 ± 0.35 mm in length, and "short" setae are 1.50 ± 0.38 mm in length. The "long" and "short" setae exhibit an elaborate ornamentation, and a progression of structural changes is apparent along the shafts. A circumferential ridge, or annulation, divides the setal shaft into preannular and postannular parts. The preannular shaft has an irregular topography, characterized proximally by nodular protrusions and distally by longitudinally oriented, anastomosing ridges. The proximal sector of the postannular shaft is smooth-surfaced. This smooth contour gives way to a line of three (sometimes five) stout hooks and then to two rows of denticles. On the contralateral surface of the shaft, bundles of foliate setules align with the hooks, and a continuous band of foliate setules parallels the denticles. Splaying of the two rows of denticles creates the endpiece of a seta. This pattern of setal ornamentation is considerably more elaborate than any previously attributed to decapod crustaceans.

The first three thoracopods (maxillipeds) of a decapod crustacean act in concert with other feeding and ventilatory appendages of the head (Pearson, 1908). Modified appendages form the floor of the prebranchial chamber, manipulate food, and often perform sensory roles. A flabellum ("gill raker" or epipodite) originates from the posterior aspect of each maxilliped. The inner surfaces of the flabella adjoin the gills, and the outer surfaces border the walls of the branchial chamber. The rounded edges of the flabellar blades are fringed with setae.

The flabella extend posteriorly into the branchial chamber for variable distances, being situated between the gills and the branchiostegite (a downgrowth of the carapace that forms the roof and lateral wall of the branchial chamber) or between the gills and the medial wall of the branchial chamber. Flabellar setae ostensibly clean the gills and the walls of the branchial chamber. In the absence of the first flabellum, the gills become covered with a layer of muddy silt (Pearson, 1908), indicating that many particles trapped by the branchial lamellae cannot be dislodged by water currents alone.

In this report, we provide a morphological description of the flabella of the green shore crab *Carcinus maenas*, as revealed by scanning electron microscopy. We illustrate an elaborate ornamentation of the flabellar setae and present

[1] This project was supported by Research Operating Grants OGP00000484 (M.J.C.) and OGP0005494 (J.L.W.) from the Natural Sciences and Engineering Research Council (NSERC) of Canada. Mr. Modi was supported by an NSERC Undergraduate Student Research Award.

TRANS. AM. MICROSC. SOC., 111(1): 16–27. 1992.

a morphometric comparison of the "long" and "short" setal variants. Portions of this investigation are reported in abstract form (Cavey et al., 1992).

Materials and Methods

Green shore crabs (*Carcinus maenas* L.) were obtained from the Marine Biological Laboratory (Woods Hole, Massachusetts, U.S.A.). The adult specimens were maintained in refrigerated tanks containing artificial seawater.

Prior to surgical exposure of the branchial chamber, animals were anesthetized by chilling to 1°C. The legs were induced to autotomize by applying pressure to the meropodite-coxopodite joint. The ventral and lateral margins of the branchiostegite were clipped away, revealing the gills and flabellum 1. For photomacrography, the crab was mounted in a bath of aerated seawater. It was photographed with a Minolta SRT-200 single-lens reflex camera equipped with a wide-field lens and an electronic flash unit. Photomacrographs were made on Kodak Panatomic-X® film.

For scanning electron microscopy (SEM), after exposure of the branchial chamber as described above, the flabella were flooded *in situ* with a fixative consisting of 2.5% glutaraldehyde, 0.2 M Millonig's phosphate buffer (pH 7.4), and 0.14 M sodium chloride (Cloney & Florey, 1968). Maxillipeds 1, 2, and 3 were excised and placed in containers of fresh fixative for 45–60 min at ambient temperature. The fixed specimens were washed with several changes of 0.1 M Millonig's phosphate buffer (pH 7.4) for 30–45 min. Particulate debris and coagulated blood cells adhering to the specimens were dispersed by intermittent ultrasonication for a total of 30–45 sec. The maxillipeds were dehydrated slowly in graded solutions of ethanol and dried in a Bomar SPC-900/EX critical-point apparatus using carbon dioxide as the transitional fluid. The flabella then were separated from the maxillipeds and cut into shorter lengths with razor blades. Flabellar segments were secured to aluminum stubs with double-sided cellophane tape and coated with a gold-palladium film, approximately 25 nm in thickness, in a Polaron E5000C sputtering system. Specimens were examined and photographed with a JEOL JSM-35CF scanning electron microscope at an accelerating voltage of 10 kV. The instrument was calibrated with screens and gratings of known spacings (16, 59, and 600 lines/mm). Micrographs were made on Ilford FP4 film.

Setae for morphometric analysis were plucked from the dried flabella with fine forceps and mounted flat on stubs for scanning electron micrography. After assembling the micrographs into montages, the morphological landmarks were identified, and the lengths of nine sectors of the setal shaft were measured. Ten "long" setae and 10 "short" setae were analyzed in this manner. Mean lengths and standard deviations were calculated for the two setal categories and for the nine defined sectors along their shafts.

Results

All branchial flabella of *Carcinus maenas* arise from the protopodites of the maxillipeds (Fig. 1). Flabellum 1 is an elongate, paddle-shaped structure that originates near the anteromedial boundary of the branchial chamber (Fig. 2).

Setae do not appear on the initial segment of the flabellum, but they may be found on both major subdivisions (coxopodite and basipodite) of the protopodite. Flabellum 1 runs the entire length of the branchial chamber, being situated between the nine phyllobranchiate gills (Goodman & Cavey, 1990) and the branchiostegite. The dorsoventral sweep of this flabellum ranges from the bases to the tips of the gills that rest against the medial wall of the branchial chamber. The broad surfaces of the blade appose the gills and the branchiostegite, and the rounded edges of the blade are fringed with setae (Fig. 3). A raphe is evident in the longitudinal midline on the external surface of the blade.

Flabella 2 and 3 (Fig. 1) also have the appearance of flattened paddles with rounded edges and setal fringes. They project between the gills and the medial wall of the branchial chamber, and their sweeps are restricted to the inside surfaces of select anterior gills. Flabellum 3 is located below flabellum 2 and extends slightly farther posteriorly. Protopodites of maxillipeds 2 and 3 also give rise to (podobranch) gills 1 and 3, respectively. Gill 1 (Fig. 2) is directed posteriorly, rather than dorsally, and gill 3 (Fig. 1) is embedded in the base of (arthrobranch) gill 5 (Pearson, 1908).

Two populations of bacteria adhere to the flabellar cuticle. These bacteria, identical to those already described on the surfaces of the branchial lamellae (Goodman & Cavey, 1990), impart a patchiness to the appearance of the cuticle (Figs. 3, 4). Lighter areas correspond to aggregations of digitiform ("rod") bacteria, and darker areas may be attributed to the presence of closely packed, short ("square") bacteria. Owing to the prevalence of bacteria within the branchial chamber, very little cuticular surface area is exposed directly to the seawater environment.

→

FIG. 1. Protopodite of maxilliped 3, showing the origins of gill 3 (g3) and flabellum 3 (f3); SEM. cx, coxopodite. Scale bar represents 1 mm. FIG. 2. Photomacrograph of an adult crab after partial removal of the wall (arrowhead) of the left branchiostegite. Flabellum 1 (f1) originates from the protopodite of maxilliped 1 and extends over the phyllobranchiate gills. Gill 1 (g1) arises from maxilliped 2. p, pereiopods. Scale bar represents 1 cm. FIG. 3. Flattened blade of flabellum 1 (f1); SEM. Numerous setae (s) emerge from the rounded edges of the blade. Scale bar represents 0.5 mm.

FIG. 4. Surface of flabellum 1; SEM. "Rod" bacteria (rb) and "square" bacteria (sb) account for the light and dark patches, respectively, on the flabellar cuticle. Scale bar represents 100 μm. FIG. 5. Proximal sector of the preannular shaft; SEM. Note the articulation (a) where the seta (s) emerges from the socket in the flabellum (f1) and the nodular protrusions (arrowheads) of the setal shaft. Scale bar represents 10 μm. FIG. 6. Distal sector of the preannular shaft; SEM. Interconnected longitudinal ridges distinguish the setal shaft in this sector. Scale bar represents 10 μm. FIG. 7. Proximal sector of the postannular shaft; SEM. The setal shaft has a smooth surface in this sector. Scale bar represents 10 μm.

FIG. 8. Distal subterminal sector of the postannular shaft; SEM. Unilateral clusters of foliate setules (fs) align in series. Scale bar represents 5 μm. FIG. 9. Foliate setules from subterminal clusters along the seta; SEM. Each setule is articulated (arrowhead) to the setal shaft. Scale bar represents 1 μm. FIG. 10. Distal subterminal sector of the postannular shaft; SEM. Contralateral to the clusters of foliate setules (cf. Fig. 8), three stout hamate setules (hs), represented by a cleat-like structure and two cornuted hooks, are evident. The cornuted hooks point toward the annulation of the seta. ds, denticulate setule; fs, foliate setule. Scale bar represents 10 μm.

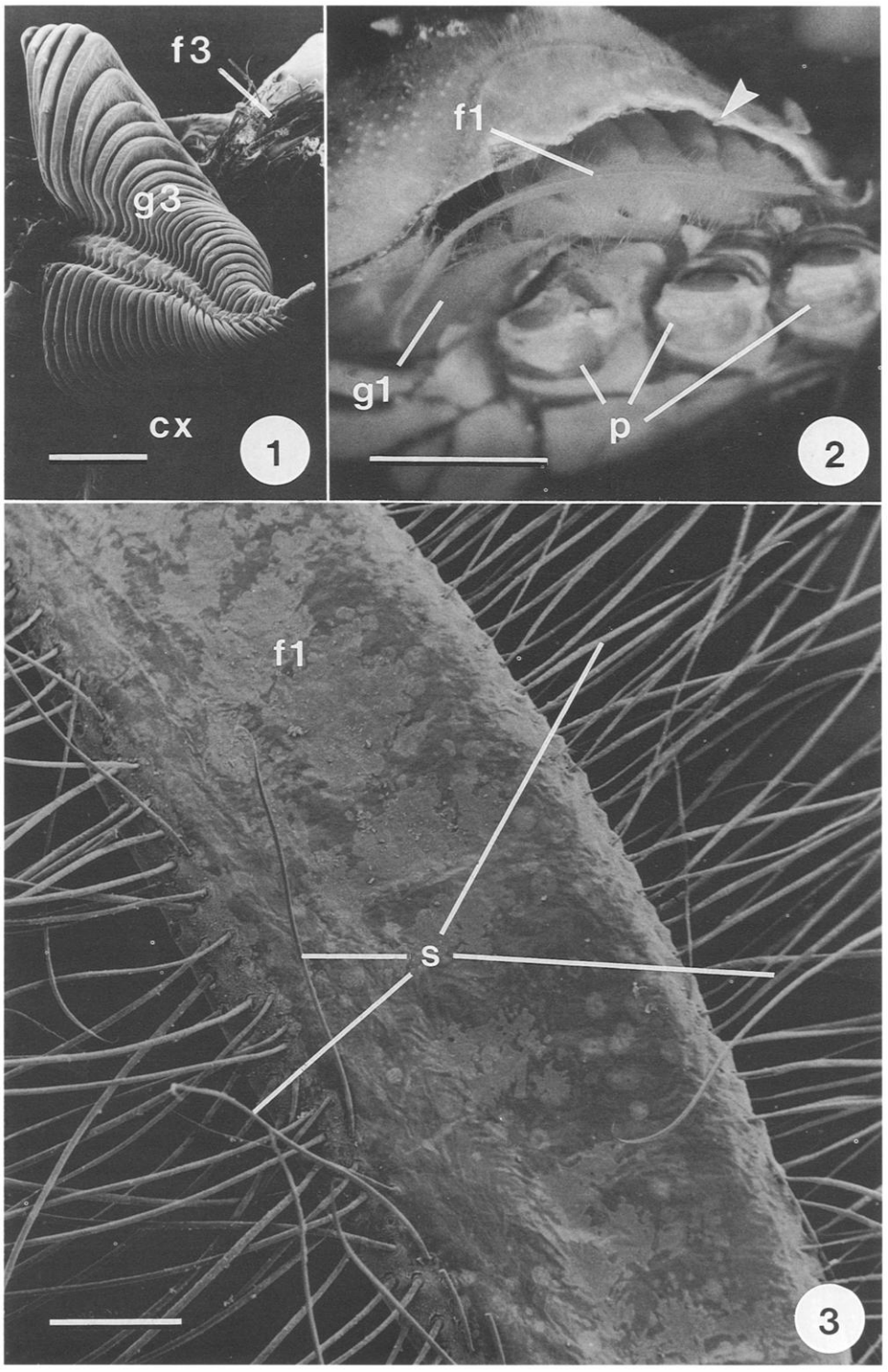
f3
g3
cx
1
f1
g1
p
2
f1
s
3

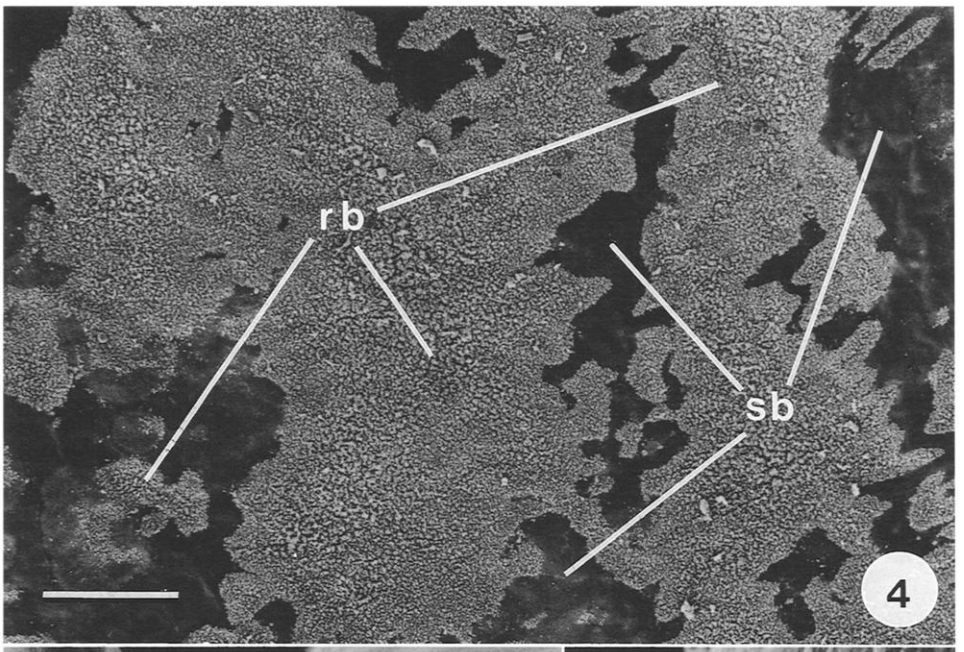
rb
sb
4

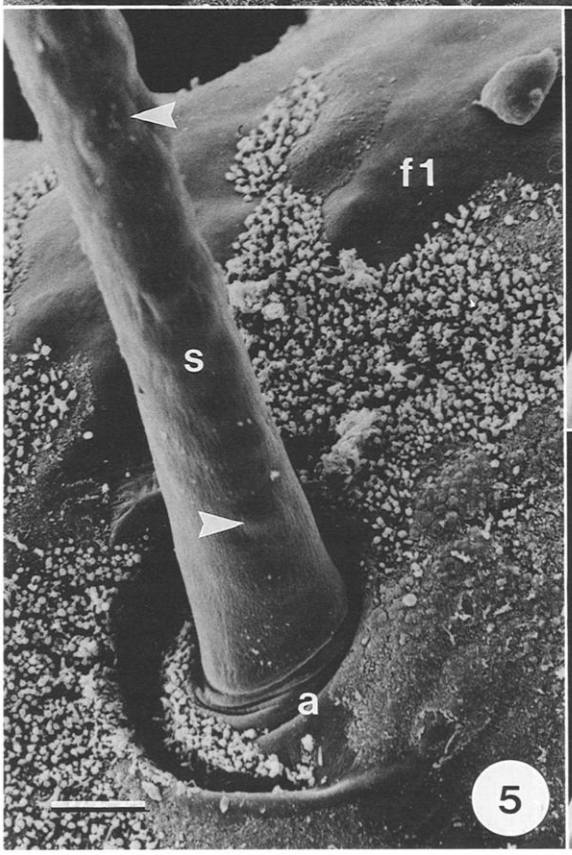
f1
s
a
5

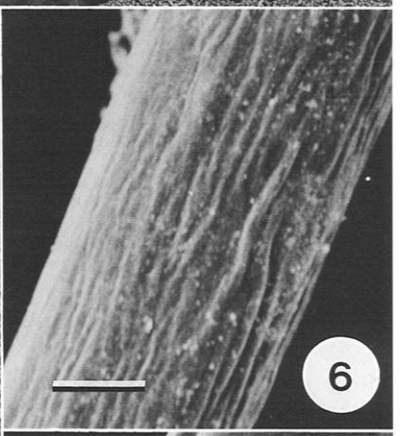
6

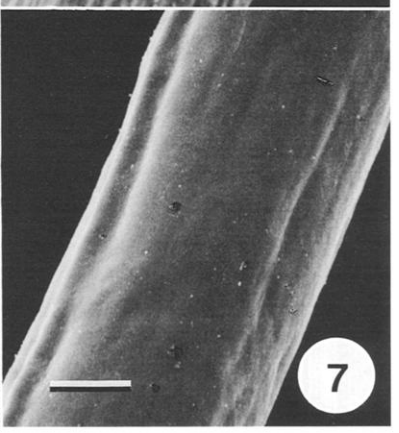
7

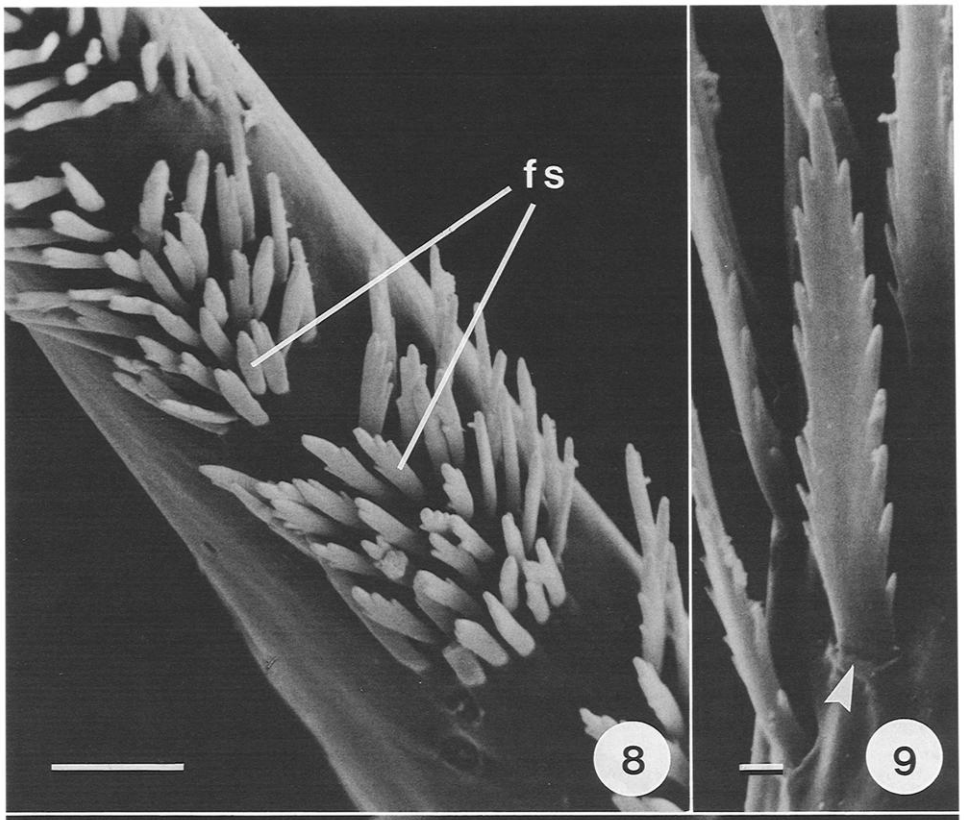
fs
8

9

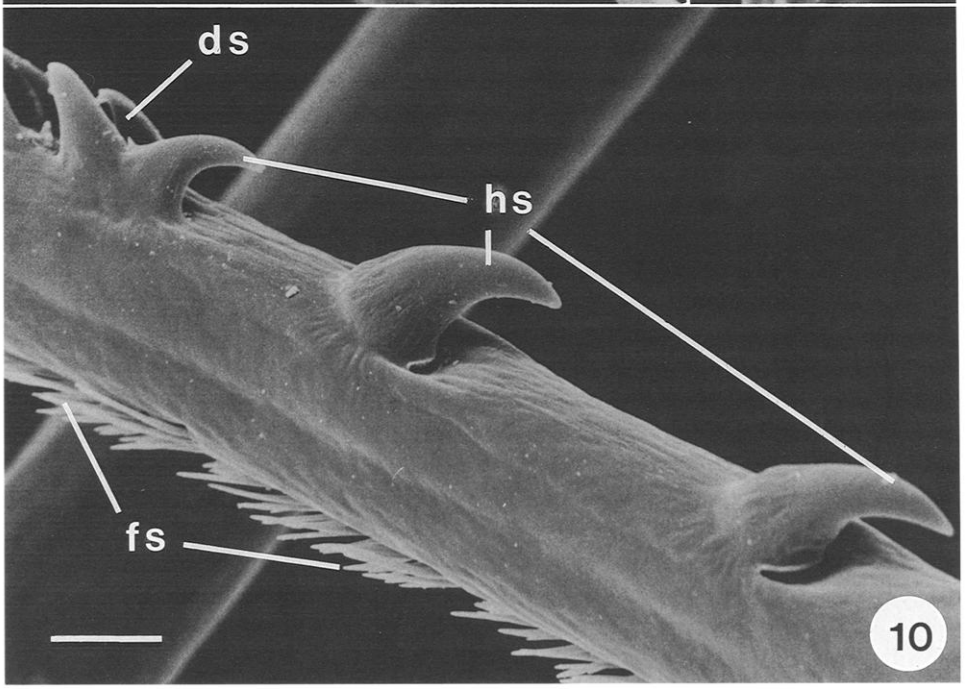
ds
hs
fs
10

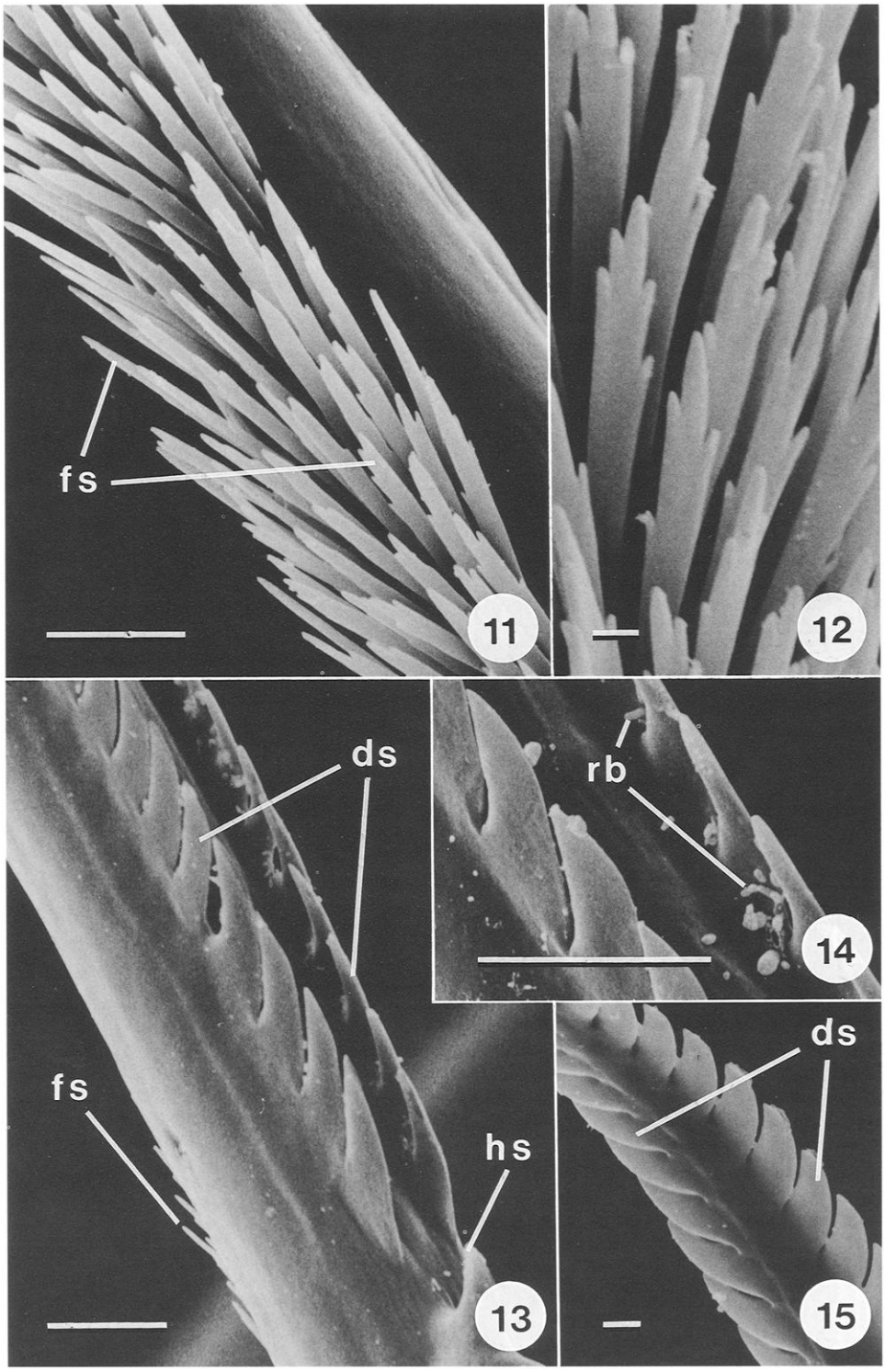
fs
11
12
ds
rb
14
fs
hs
13
ds
15

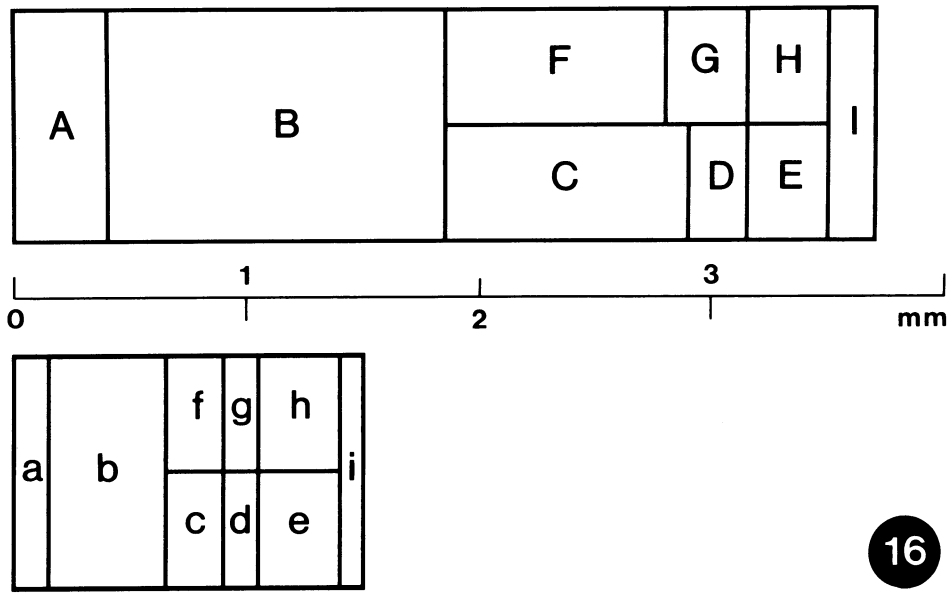

FIG. 16. Diagrammatic representations of the mean lengths of the morphological sectors along the "long" (top) and "short" (bottom) setae of the flabella. Letter codes for the nine sectors of the setal shaft (A-I for "long" setae and a-i for "short" setae) are explained in the footnote to Table I.

Several rows of setae appear on the rounded edges of the flabellar blade (Fig. 3). Each seta emerges from a socket that is a shallow cuticular invagination (Fig. 5). The sockets are angled relative to the flabellar surface so that the setae emerge obliquely from the blade. These features would indicate that the seta is a flexible projection, but one that is constrained in its freedom of movement. Proximal regions of the setal shaft are hollow, a finding verified both by natural breaks and intentional fractures.

Setae range in length from about 1.1 mm to about 4.2 mm, but, regardless of length, they exhibit a number of discrete sectors that may be defined morphologically (Table I). The shaft, which tapers terminally to a point, is divided

---

←

FIG. 11. Distal subterminal sector of the postannular shaft; SEM. The discrete clusters of foliate projections (cf. Fig. 9) are replaced by a continuous band of setules (fs). Scale bar represents 5 μm. FIG. 12. Foliate setules from the subterminal band along the seta; SEM. These setules are somewhat simpler in morphology than their counterparts from the discrete clusters (cf. Fig. 9). Scale bar represents 1 μm. FIG. 13. Distal subterminal sector of the postannular shaft; SEM. Immediately beyond the cleat-like member (hs) of the hamate trio, two rows of denticulate setules (ds) appear. The denticles point toward the tip of the seta. fs, foliate setule in the longitudinal band. Scale bar represents 10 μm. FIG. 14. Denticulate setules and the intervening depression; SEM. "Rod" bacteria (rb) adhere to the elevated structures. Scale bar represents 10 μm. FIG. 15. Scanning electron micrograph of a distal terminal sector of the postannular shaft; SEM. The parallel rows of denticulate setules (ds) turn outward, becoming the lateral borders of the endpiece of the seta. Scale bar represents 1 μm.

TABLE I

Morphometry of the "long" and "short" flabellar setae of *Carcinus maenas*

	Length (μm) by sector*									
	A	B	C	D	E	F	G	H	I	Total
"Long" setae	0.41	1.65	1.22	0.38	0.33	1.22	0.43	0.27	0.19	4.17
	0.43	1.79	1.14	0.33	0.22	1.17	0.30	0.22	0.30	4.20
	0.46	1.25	1.06	0.22	0.35	0.81	0.41	0.41	0.19	3.52
	0.43	1.65	1.06	0.27	0.35	0.87	0.46	0.35	0.22	3.99
	0.38	1.30	1.03	0.24	0.38	0.89	0.35	0.41	0.22	3.55
	0.46	1.60	0.98	0.24	0.33	0.81	0.41	0.33	0.22	3.82
	0.41	1.08	0.79	0.27	0.27	0.49	0.46	0.38	0.16	2.98
	0.41	1.36	0.76	0.24	0.46	0.79	0.35	0.33	0.24	3.47
	0.38	1.55	1.08	0.24	0.33	0.95	0.46	0.24	0.27	3.85
	0.38	1.41	1.11	0.24	0.30	0.98	0.35	0.33	0.22	3.66
Mean	0.41	1.46	1.02	0.27	0.33	0.90	0.40	0.33	0.22	3.72
Standard deviation	0.03	0.21	0.14	0.05	0.06	0.19	0.05	0.06	0.04	0.35
	a	b	c	d	e	f	g	h	i	Total
"Short" setae	0.24	0.70	0.19	0.14	0.35	0.19	0.24	0.24	0.14	1.76
	0.16	0.57	0.22	0.14	0.27	0.14	0.24	0.24	0.11	1.46
	0.19	0.68	0.24	0.14	0.35	0.22	0.19	0.33	0.11	1.71
	0.10	0.32	0.22	0.10	0.30	0.20	0.15	0.27	0.10	1.13
	0.12	0.27	0.20	0.07	0.32	0.20	0.12	0.27	0.10	1.08
	0.15	0.35	0.25	0.07	0.32	0.20	0.12	0.32	0.10	1.23
	0.15	0.35	0.17	0.10	0.30	0.17	0.15	0.25	0.10	1.16
	0.12	0.35	0.25	0.10	0.35	0.20	0.12	0.37	0.10	1.26
	0.20	0.58	0.34	0.17	0.47	0.30	0.24	0.44	0.14	1.90
	0.34	0.71	0.41	0.20	0.47	0.41	0.24	0.44	0.17	2.30
Mean	0.18	0.49	0.25	0.12	0.35	0.22	0.18	0.32	0.12	1.50
Standard deviation	0.07	0.17	0.07	0.04	0.07	0.07	0.05	0.07	0.02	0.38

* Preannular shaft: A, a proximal sector with nodular protrusions (cf. Fig. 5); B, b distal sector with longitudinal ridges (cf. Fig. 6). Postannular shaft: C, c proximal sector with smooth surface (cf. Fig. 7); D, d distal subterminal sector with hamate setules (cf. Fig. 10); E, e distal subterminal sector with two rows of denticulate setules (cf. Fig. 13); F, f distal subterminal sector with smooth surface (cf. Fig. 7); G, g distal subterminal sector with clusters of foliate setules (cf. Fig. 8); H, h distal subterminal sector with band of foliate setules (cf. Fig. 11); I, i distal terminal sector representing setal endpiece (cf. Fig. 15).

into two parts by an annulation (Thomas, 1970). The proximal sector of the preannular shaft displays a number of nodular protrusions arranged in a spiral pattern (Fig. 5). These nodules of the preannular shaft quickly give way to a network of longitudinally oriented, anastomosing ridges (Fig. 6). The ridges end abruptly at the annulation, and the proximal sector of the postannular shaft is smooth-surfaced (Fig. 7). The distal, subterminal sector of the postannular shaft is lavishly ornamented. Several types of setules may be identified in contralateral positions. Three stout hamate setules occur in a line on one side of the shaft (Fig. 10). The most distal member of this trio is cleat-shaped, and the tips of the two cornuted hooks are directed toward the annulation. (On

some setae, five hooks appear in the customary position of the three hamate setules. All five hooks, in such cases, are curved toward the annulation.) On the opposite side of the shaft, but closely aligned with the hooks, are several clusters of foliate setules (Figs. 8, 9).

Beyond the cleat-like hook, a shallow groove appears and extends toward the free end of the seta (Fig. 13). This groove is flanked on either side by a row of denticulate setules. The apices of these denticles are directed toward the setal tip (Fig. 14). As the diameter of the shaft decreases, the rows of denticles begin to splay laterally and the intervening groove becomes progressively more shallow. Each row of setules ultimately turns through an arc of approximately 90°. When splaying is complete, the two rows form the sides of the setal endpiece (Fig. 15). The clusters of foliate setules, aligned with the three (or five) hooks, are supplanted gradually by a continuous band of projections (Figs. 11, 12). The setules in this longitudinal band retain a foliate appearance, but they generally possess fewer pinnae than those in the clusters. The band of foliate setules may be followed to the level where the rows of denticles begin to splay.

The flabellar setae, on the basis of length, fall into two categories: the "long" setae are 3.72 ± 0.35 mm in length and the "short" setae are 1.50 ± 0.38 mm in length (Table I). The extents of the morphological sectors along the "long" and "short" setae are summarized in the diagrams of Fig. 16.

Discussion

The last pair of cephalic appendages (maxillae 2) form the scaphognathites ("gill balers"). By dorsoventral movements within the confined spaces of the prebranchial chambers, the scaphognathites pull seawater into the branchial chambers and across the gills (Paterson, 1968). Recent studies that chart the seawater movements in the branchial chamber report no evidence of flabellar involvement in either pumping water or directing currents (Hughes et al., 1969; Wilkens & McMahon, 1972). The potential role of flabella as accessory organs to the scaphognathites, therefore, seems remote.

Pumping actions of the scaphognathites move seawater into the branchial chambers in a posterior-to-anterior direction. At irregular intervals, reversal beats occur, propelling water backward (Hughes et al., 1969; Wilkens & McMahon, 1972). The purpose of reversal beats is unresolved: they might (1) ensure the proper irrigation of posterior gills (Arudpragasam & Naylor, 1964a,b); (2) flush detritus from the surfaces of the posterior gills (Arudpragasam & Naylor, 1966; Hughes et al., 1969); or (3) purge foreign matter from the sensory hairs in the vicinity of the branchiostegite (Wilkens & McMahon, 1972). Reversal beats also could represent stereotyped responses of the organism when it encounters extraordinary stimuli (Wilkens & McMahon, 1972), such as mechanical stimulation of the gills (Rajashekhar & Wilkens, 1991).

If reversal beats do indeed flush detritus from the branchial lamellae, the scaphognathites might be acting cooperatively with the flabella. Other branchial and peribranchial setae of a crab also deter fouling of the gills. For example, setae along the posterior border of maxilliped 3 and at the anterior face of

thoracopod 4 (chela or pereiopod 1) are positioned suitably to strain the seawater as it enters the branchial chamber (Pearson, 1908).

A considerable amount of information on setal morphology and classification in decapod crustaceans has come from investigations on crayfish. In a comprehensive study of *Austropotamobius pallipes* using light microscopy, Thomas (1970) recorded many variations among the setae on the body and the appendages and devised a classification scheme based on external shape, relative size, terminal structure, cuticularization of the shaft, and branches and serrations of the surface. All setae of *A. pallipes* arise from sockets, and each possesses an apical pore that opens either terminally or subterminally. Two principal groups of setae were recognized in *A. pallipes*. Aseptate setae are thick-walled structures with narrow lumina, and they lack both a conspicuous ampulla (a dilated segment of the shaft adjacent to the socket) and a basal septum (a circular thickening of the wall at the junction of the ampulla and shaft proper). Septate setae, on the other hand, are thin-walled structures with wide lumina that possess both prominent ampullae and basal septa. A subsequent examination of crayfish hatchlings (Thomas, 1973) revealed that all early setae could be allied with operation of the branchial chambers, including the hamate setae of the chelae, maxillipeds, and pereiopods (walking legs), as well as the pappose setae of the carapace, scaphognathites, and maxillipeds.

Studies of the mouthparts of lobsters, in both the larvae of *Homarus americanus* (see Factor, 1978) and the adults of *Nephrops norvegicus* (see Farmer, 1974), again illustrate extreme variations in setal form, which, in turn, hamper construction of valid schemes for classification. In lobsters, setae of the mouthparts might affect water currents in the branchial chambers in several ways: (1) certain setae might amplify the surface areas of the scaphognathites to increase their pumping efficiency; (2) other setae might seal the spaces between maxillae 2 and the medial walls of the branchial chambers to bolster pumping efficiency of the scaphognathites; (3) setae along the margins of the branchial chambers might filter incoming seawater to block the entry of larger particles; and (4) setae on the maxillipeds, which do not form flabella, might sweep away particles that foul the gills and branchial chambers.

Functional assessments of the branchial flabella of *Carcinus maenas* are feasible in the laboratory. For long-term observations, a branchial chamber may be exposed and the branchiostegite may be replaced with a thin sheet of plastic that has been heat-molded to the contours of the carapace (Hughes et al., 1969). By suspending progressively smaller sizes of charcoal particles in seawater, perhaps the size limit of detritus that can be cleared effectively by the flabellar seta may be determined. High-speed video analysis holds promise for analyzing the dorsal and ventral strokes of flabellum 1 and for observing the behavior of its setae relative to the surfaces of gills 5–9 and the inner aspect of the branchiostegite.

Literature Cited

ARUDPRAGASAM, K. D. & NAYLOR, E. 1964a. Gill ventilation and the role of reversed respiratory currents in *Carcinus maenas* (L.). *J. Exp. Biol.*, 41: 299–307.

1964b. Gill ventilation volumes, oxygen consumption and respiratory rhythms in *Carcinus maenas* (L.). *J. Exp. Biol.*, 41: 309–321.

1966. Patterns of gill ventilation in some decapod Crustacea. *J. Zool. (London)*, 150: 401–411.

CAVEY, M. J., MODI, E. & WILKENS, J. L. 1992. Ornate setae on the branchial flabella of a decapod crustacean. (Abstr.) *Trans. Am. Microsc. Soc.*, 111: 73.

CLONEY, R. A. & FLOREY, E. 1968. Ultrastructure of cephalopod chromatophore organs. *Z. Zellforsch. Mikrosk. Anat.*, 89: 250–280.

FACTOR, J. R. 1978. Morphology of the mouthparts of larval lobsters, *Homarus americanus* (Decapoda: Nephropidae), with special emphasis on their setae. *Biol. Bull. (Woods Hole)*, 154: 383–408.

FARMER, A. S. 1974. The functional morphology of the mouthparts and pereiopods of *Nephrops norvegicus* (L.) (Decapoda: Nephropidae). *J. Nat. Hist.*, 8: 121–142.

GOODMAN, S. H. & CAVEY, M. J. 1990. Organization of a phyllobranchiate gill from the green shore crab *Carcinus maenas* (Crustacea, Decapoda). *Cell Tissue Res.*, 260: 495–505.

HUGHES, G. M., KNIGHTS, B. & SCAMMELL, C. A. 1969. The distribution of P_{O_2} and hydrostatic pressure changes within the branchial chambers in relation to gill ventilation of the shore crab *Carcinus maenas* L. *J. Exp. Biol.*, 51: 203–220.

PATERSON, N. F. 1968. The anatomy of the Cape rock lobster, *Jasus lalandii* (H. Milne-Edwards). *Ann. S. Afr. Mus.*, 51: 1–232.

PEARSON, J. 1908. *Cancer. In* Herdman, W. A., ed., *Liverpool Marine Biology Committee Memoirs on Typical British Marine Plants & Animals*, No. XVI, Williams & Norgate, London, pp. 1–209.

RAJASHEKHAR, K. P. & WILKENS, J. L. 1991. Control of 'pulmonary' pressure and coordination with gill ventilation in the shore crab *Carcinus maenas*. *J. Exp. Biol.*, 155: 147–164.

THOMAS, W. J. 1970. The setae of *Austropotamobius pallipes* (Crustacea: Astacidae). *J. Zool. (London)*, 160: 91–142.

1973. The hatchling setae of *Austropotamobius pallipes* (Lereboullet) (Decapoda, Astacidae). *Crustaceana*, 24: 77–89.

WILKENS, J. L. & MCMAHON, B. R. 1972. Aspects of branchial irrigation in the lobster *Homarus americanus*. I. Functional analysis of scaphognathite beat, water pressures and currents. *J. Exp. Biol.*, 56: 469–479.